

Solid State NMR Investigation of Cationic Polymerized Epoxy Resins

N. EGGER,¹ K. SCHMIDT-ROHR,¹ B. BLÜMICH,¹ W.-D. DOMKE*² and B. STAPP²

¹MPI Polymerforschung, P.O. Box 3148, D-6500 Mainz, Germany, and

²Siemens AG, ZFE ME AC 1, P.O. Box 3220, D-8520 Erlangen, Germany

SYNOPSIS

Cationic UV-polymerized resins, based on cycloaliphatic epoxides with aryl sulfonium salts as photoinitiators and polypropylene glycols of variable length as flexibilizers, have been investigated with respect to the network-forming reactions and the morphology of the resulting polymers. The combination of UV-curing and thermal postcure makes the chemical process complex and dependent on many variables, such as photoinitiator, exposure time, reaction temperature, and polyol components. Structure and curing of the epoxide were investigated by ¹³C CPMAS NMR. Morphology and domain sizes were studied by spin diffusion experiments using the novel "dipolar filter" technique for selective magnetization of mobile components.

INTRODUCTION

Epoxy resins as high-performance polymers have increasingly received interest as composite materials, protective coatings, and encapsulation materials for many electronic components.¹ Excellent thermomechanical properties and resistance against environmental influences are usually achieved by thermal crosslinking of the epoxy resin with multifunctional amines, anhydrides, or phenols as hardener components.²

In addition to thermal crosslinking, the cationic UV-polymerization of epoxy resins offers promising applications for the manufacturing of coatings, adhesives, and globe toppings in the electrical industry. The main advantages of a cationic process, as compared to a free radical process, are an insensitivity against oxygen inhibition, a smaller curing shrinkage resulting in better substrate adhesion, and the characteristics of a "living polymerization," which can be exploited in a two-step curing process.³⁻⁶

It is the resistance against solvents that makes epoxy resins difficult to analyze. Solid state NMR spectroscopy has become a powerful tool for studying

crosslinked systems with respect to chemical structure, orientation, and dynamics of specific molecular segments.^{7,8} In the study reported here, ¹³C CPMAS NMR has been used to investigate changes in mobility of UV- and thermally cured epoxy resins, structural changes, and the influence of polyol flexibilizers with variable chain length on curing rates and on polymer morphology. In particular, ¹H spin diffusion is applied with a new morphologically selective multiple pulse technique for the characterization of domain sizes.⁹

Cationic UV-Polymerization

The first step in cationic UV-polymerization of epoxy resins is the photolysis of the photoinitiator by appropriate UV-radiation, yielding strong protonic acids (HX; X = SbF₆, PF₆), which in turn initiate the opening of the epoxy rings, thus forming a polyether network.

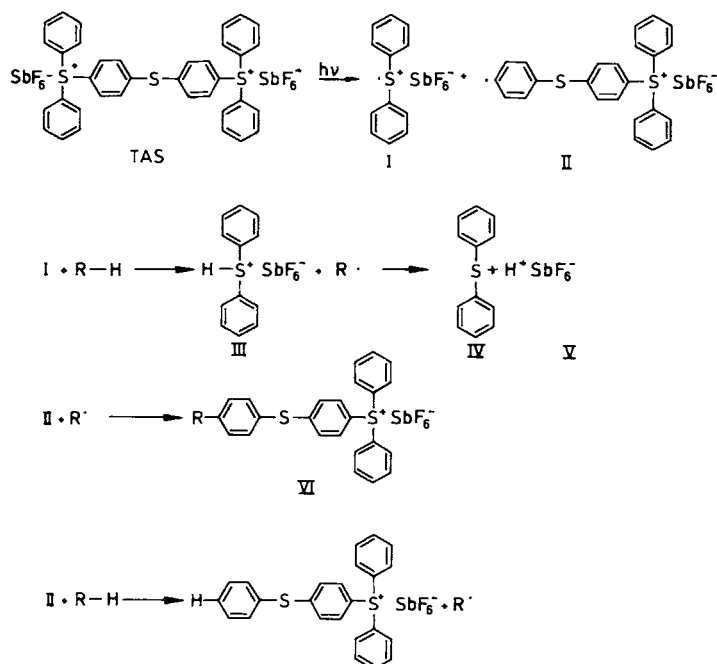
Initiation

Different initiator systems have been described for use in cationic UV-curing, that is, triarylsulfonium salts (TAS) with PF₆⁻ or SbF₆⁻-anions and areneferrocenium salts.^{4,5} These complexes are thermally stable up to 150°C. Their main UV absorbances are listed in Table I.

* To whom correspondence should be addressed.

The photolysis starts from the excited single-state⁴ by homolytic scission of a sulfur-carbon bond. Photolysis products are mainly the protonic acids

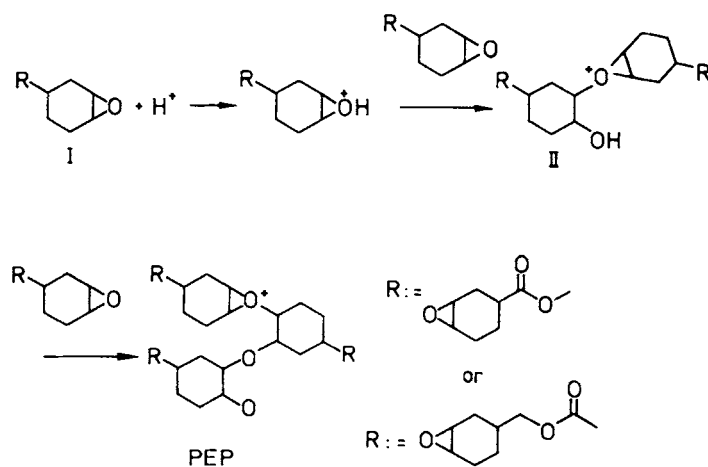
(V), diphenylsulfide (IV), and phenylthiobiphenylsulfides (VI).⁴ The protonic acids can be regarded as the actual starters of the polymerization. Quantum yields in these systems are known to be high.¹⁰



Propagation

The polymerization of the neat epoxy component 3,4-epoxy-cyclohexylmethyl-3',4'-epoxycyclohexanecarboxylate (I) starts by cationic ring opening

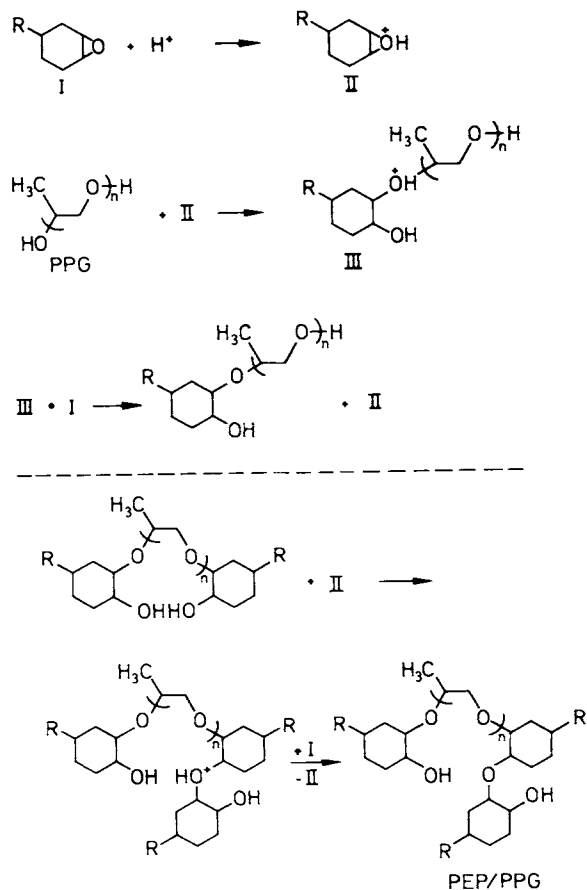
polymerization. Polymerization yields a three-dimensional network of polyether structures (PEP). The polymerization centers are the tertiary oxonium ions (II) in the growing polymer.



Introduction of polypropylene glycol (PPG) flexibilizers shifts the reaction pathway to an "activated monomer mechanism," where the polymerization is supported by a protonated epoxy monomer (II).

This has been shown for systems of cyclic acetals and alcohols by Penczek.¹¹ This chain transfer reaction will significantly influence the curing rates

as well as the number of chain terminations, and therefore the morphology and the thermo-mechanical properties of the network.



Termination

In contrast to radical reactions, there is no termination but a more or less reversible blocking of the cationic centers by nucleophilic impurities. Part of the cations may remain active over a long period of time.

EXPERIMENTAL

Samples

Five samples of PEP with different flexibilizer content were prepared. The epoxide was obtained from Degussa AG (Degacure K 126), and the flexibilizer from Aldrich (polypropylene glycol). All monomers were used without further purification. The samples and their abbreviations are identified in Table II.

Three samples exhibited different degrees of polymerization of the polypropylene glycol. In the other two, the amount of flexibilizer was varied. A sample of 0.5% Photoinitiator (Degacure KI, De-

Table I UV Absorbances of Photo-Initiator Complexes (TAS)

Wavelength [nm]	Absorbances ϵ ($1 \text{ mol}^{-1}\text{cm}^{-1}$)
275	18,633
284	18,490
315	17,920

gussa AG) was dissolved in the epoxide and then was placed into a quartz sample tube. To initiate the reaction, the mixture was exposed to UV-light (Hoenle UV-A Spot, 20 mW/cm^2) for a duration as long as 5 min. The sample temperature did not exceed 50°C during UV-irradiation. All samples were polymerized in quartz tubes of appropriate diameter to fit tightly in the NMR-MAS rotors.

NMR Experiments

All spectra were acquired on a Bruker MSL 300 spectrometer with solid state NMR accessories using a 90° -proton pulse width of $4.0 \mu\text{s}$. The experiments did not require dedicated multiple pulse tuning of the spectrometer.

RESULTS AND DISCUSSION

^{13}C CPMAS Measurements

All samples were amorphous and transparent, except for the sample PEP/PPG₁, which was opaque. The ^{13}C CPMAS spectrum of the PEP homopolymer is shown in Figure 1(a) two weeks after preparation. The spinning sidebands are marked by SSB. The signal at 51 ppm is assigned to carbons of the unreacted epoxy groups. Within a period of 9 months this peak totally disappears [Fig. 1(b)].

Figure 1(c) depicts the spectrum of the PEP/PPG copolymer directly after preparation. No signals from monomer are visible. The methyl peak gives one extra signal at 18 ppm in addition to the PEP spectrum in Fig. 1(a). The conversion of the epoxide in the PEP/PPG system is higher than for the homopolymerization of the epoxide. Further, the reaction rate of the two component system was faster than that of the homopolymerization.

Morphology by Multiple Pulse Spin Diffusion Experiments

NMR can be used to study domain sizes by monitoring spin diffusion.¹²⁻²⁵ Initially a spatial magne-

Table II Investigated PEP/PPG Samples

Notation	Degree of Polymerization of PPG	Ratio of EP : PPG (by Weight)
PEP/PPG _a	17	2, 0 : 1
PEP/PPG _m	35	2, 0 : 1
PEP/PPG ₁	70	2, 0 : 1
PEP/PPG _{m2}	35	1, 3 : 1
PEP/PPG _{m3}	35	2, 7 : 1

tization gradient is established in the proton spin system by application of a special multiple pulse sequence. The equilibration of this gradient by ^1H spin diffusion is followed as a function of time. Given the spin diffusion constant of ^1H ($D = 0.002 - 0.7 \times 10^{-15} \text{ m}^2/\text{s}$), domain sizes in the heterogeneous materials reported here can be estimated from the signal build-up as a function of the spin diffusion time.²⁶⁻²⁹ This experiment parallels the well-known Goldman-Shen sequence with ^{13}C -detection.^{30,31} There, a magnetization gradient is established by exploiting differences in relaxation times of, e.g., crystalline (rigid) or amorphous (mobile) domains in semicrystalline materials. However, problems originating in the excitation of multiple quantum coherences are known to arise with the Goldman-Shen sequence for short spin diffusion times.³²

The sequence used here employs the "dipolar filter"⁹ for selective polarization of mobile protons. The sequence can be used for short as well as long diffusion times, since multiple quantum transitions are not excited. After the filter, the magnetization is allowed to equilibrate for a spin diffusion time t_m (Fig. 2). For detection, the ^1H magnetization is cross-polarized to ^{13}C in order to exploit the large chemical shift scale of ^{13}C for identification of the magnetization sinks.³¹

The pulse sequence of the "dipolar filter" is depicted in Figure 3. This multiple pulse sequence is designed to average all interactions (dipolar couplings as well as the chemical shift) of the protons. However, the windows τ between the pulses are not kept short as usual, but are set to rather long values of 7–20 μs . As a result, the averaging is not effective for large dipolar couplings and the magnetization of the corresponding protons relaxes. The remaining magnetization belongs to protons where the dipolar coupling is small, as a result of partial averaging due to high molecular mobility. In this way only the mobile regions of the sample are magnetized after application of the dipolar filter. To improve the selec-

tion, the filter pulse sequence is repeated up to 20 times.

To evaluate the sizes of the highly mobile and rigid domains, the spin diffusion equation is solved for a model of the heterogeneous material. In the case of the network of PEP and PPG, a three dimensional sphere model is used.⁹ Figure 4 shows a two dimensional cross-section of the sphere model, which defines the relevant parameters and sketches

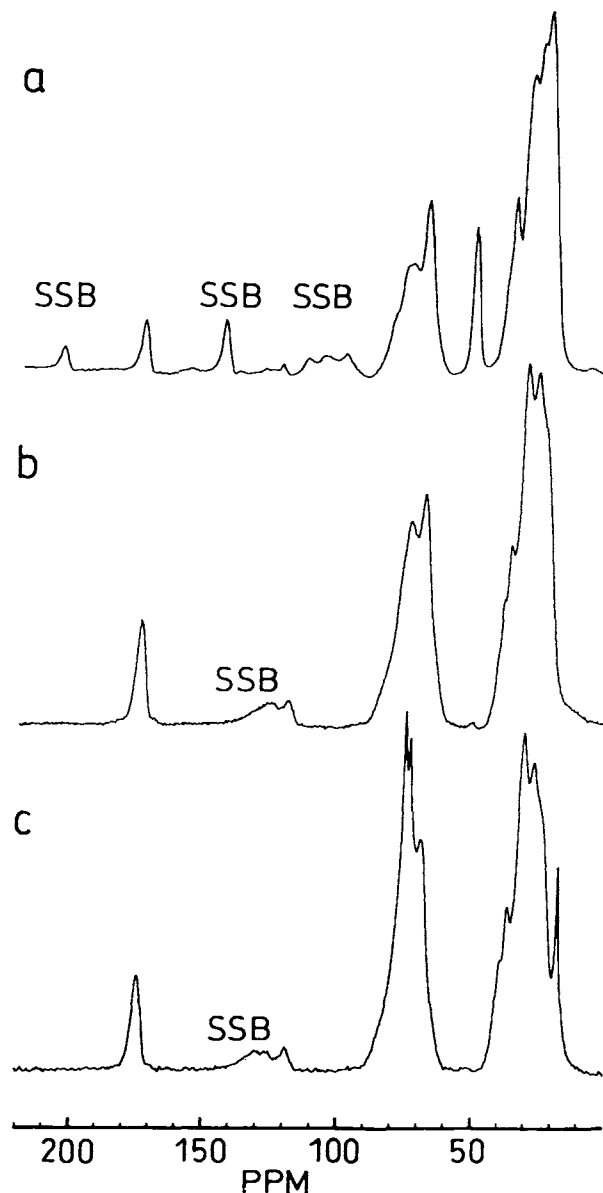


Figure 1 ^{13}C CPMAS spectra of epoxy resins: (a) PEP two weeks after preparation. At 51 ppm the signal of the unreacted epoxide is visible, (b) PEP nine month after preparation. The signal of the unreacted epoxide has disappeared, and (c) PEP/PPG two weeks after preparation.

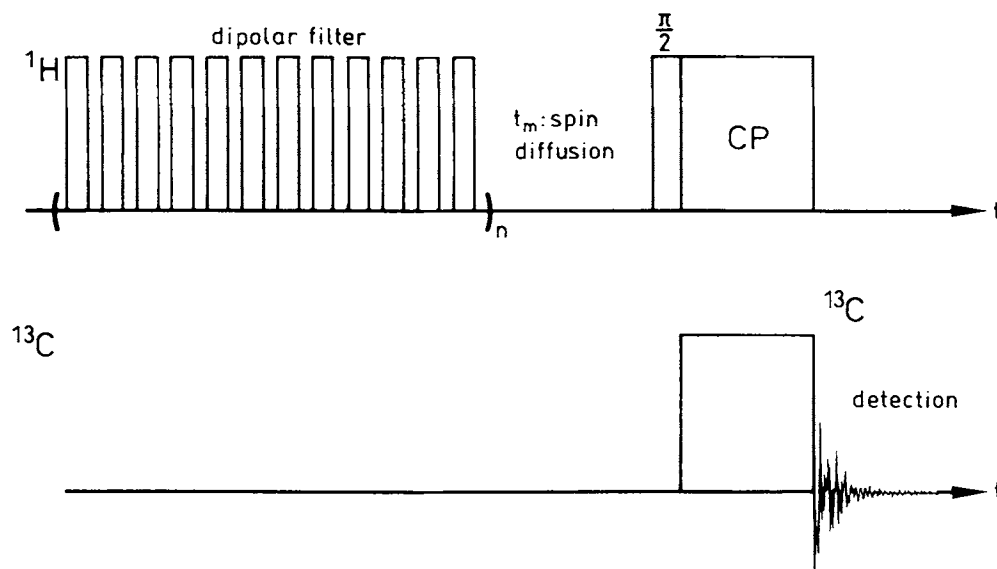


Figure 2 Dipolar filter sequence with mixing time (t_m) for ^1H spin diffusion and cross polarization for ^{13}C detection.

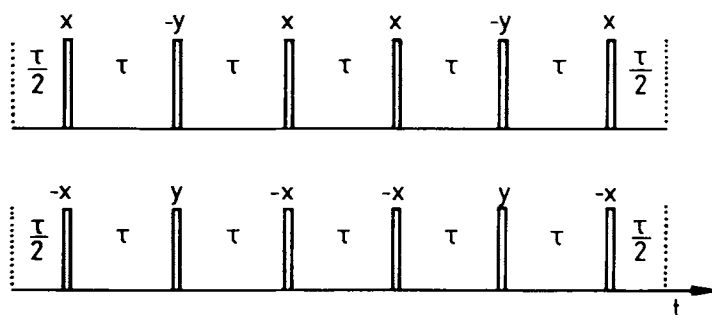


Figure 3 Pulse sequence of the dipolar filter. The sequence consists of twelve 90° -pulses.

the evolution of the magnetization as a function of the diffusion time t_m .

The experimental data for the PEP/PPG_{m2} sample and a corresponding fit are plotted in Figure 5. The error bars are derived from the errors introduced by T_1 relaxation and the uncertainty in the spin diffusion constant D . The experimental data do not

follow a straight line near the origin but rather a sigmoid curve. This indicates the existence of a small interphase made up of flexibilizer of reduced mobility.

Table III summarizes the experimental results for the diameter of the PPG (d_{PPG}) and the PEP (d_{PEP}) domains of the five samples, including the spin dif-

Table III Spin Diffusion Results

Sample	d_{PPG} (exp) (nm)	d_{PPG} (calc) (nm)	d_{PEP} (exp) (nm)	d_{ip} (exp) (nm)	D_{PPG} ($10^{-15} \text{ m}^2/\text{s}$)
PEP/PPG _s	2.1 ± 0.5	1.2	2.7 ± 0.6	0.4	0.02
PEP/PPG _m	2.6 ± 0.7	1.5	4.2 ± 1.1	0.5	0.02
PEP/PPG ₁	4.1 ± 0.5	1.9	6.5 ± 0.8	0.7	0.004
PEP/PPG _{m2}	3.1 ± 0.5	1.5	6.5 ± 1.0	0.4	0.008
PEP/PPG _{m3}	3.3 ± 0.5	1.5	6.3 ± 1.0	0.2	0.008

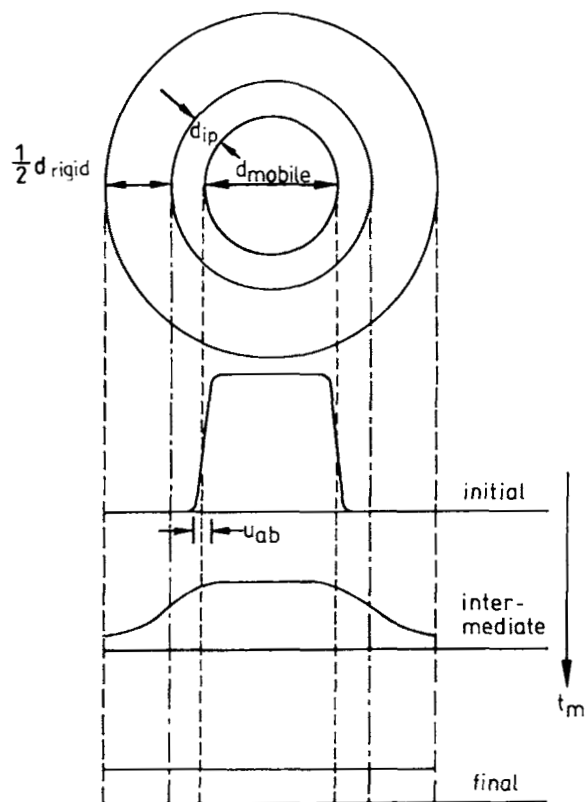


Figure 4 Cross section of the sphere model and evolution of the magnetization. See text for details.

fusion rate (D) used for simulation. The diameter of the interphase is denoted by d_{ip} (cf. Fig. 4). The details of the simulation will be described elsewhere.³³ For reference, the theoretically calculated diameters d_{PPG} (calc) of a sphere filled up by one PPG molecule with its solid state density are given. The diameter d_{PPG} includes the diameter d_{mobile} of the soft phase plus twice the size of the interphase (cf. Fig. 4). Its diameter is increasing with the degree of polymerization of the PPG. In the PEP/PPG_{m2} and PEP/PPG_{m3} samples, only the amount of flexibilizer was changed. The data in Table III show that this change has very little influence on the diameter of the PPG domains.

CONCLUSIONS

The reaction of the epoxide without flexibilizer proceeds very rapidly to its gel point. But after one day, a total conversion of only 50% is reached. The epoxide content decreases to zero in a period of over nine months, which demonstrates the rare case of a "living cationic" polymerization. The addition of PPG shifts the reaction pathway to a chain transfer reaction, which increases the curing rate and decreases the mean molecular weight. Thus gelation

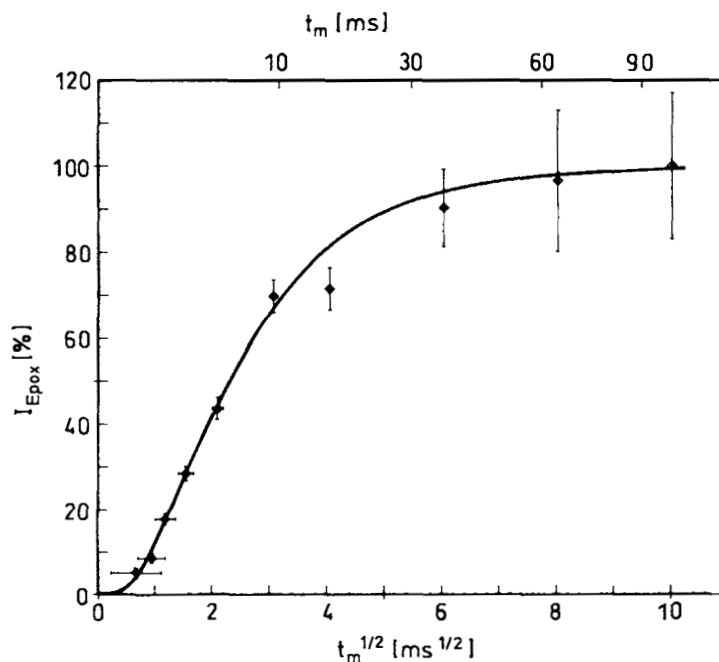


Figure 5 Intensity of the epoxy signal (19 to 44 ppm) as a function of the spin diffusion time (t_m) for the PEP/PPG_{m2} sample and corresponding fit.

is reached at higher conversion, resulting in a more complete epoxy polymerization. This follows from the ^{13}C CPMAS spectra and is in agreement with the domain sizes determined by spin diffusion measurements.

The PEP/PPG polymer is a system with micro-phase separation in which the size of the PPG phase grows as the degree of polymerization of the glycol increases. However, the PPG phase is smaller than generally expected as a consequence of the influence of the epoxide matrix. As a result of the small phase sizes, the samples are transparent. Only the PEP/PPG₁ sample, which contains very long PPG molecules (the degree of polymerization is 70), is opaque. This is explained by partial homopolymerization of the epoxide, which yields relatively large epoxide phases. In all samples, the experimentally determined phase sizes indicate that the mobile phases consist only of one or a few polyol chains.

Support of this work by Prof. Dr. H. W. Spiess (Max-Planck Institute for Polymer Research, Mainz) and Dr. H. Markert (Siemens AG, Erlangen) is gratefully acknowledged.

REFERENCES

1. F. Lohse and H. Zweifel, *Adv. in Polym. Sci.*, **78**, 61–81 (1986).
2. L. V. Mc Adams and J. A. Gannon, *Epoxy Resins*, In: *Encyclopedia of Polymer Science and Engineering*, 2nd ed., Wiley, 1986, Vol. 6, pp. 322–382.
3. M. Irie, S. Sasaoka, Y. Yamamoto, and K. Hayashi, *J. Polym. Sci.*, **17**, 815–820 (1979).
4. J. V. Crivello and J. H. W. Lam, *J. Polym. Sci.*, **17**, 977–999 (1979).
5. J. V. Crivello and J. H. W. Lam, *J. Polym. Sci.*, **56**, 383–395 (1976).
6. J. V. Crivello, *Polymer Preprints*, **25**, 235–236 (1984).
7. R. A. Komoroski, *Principles and General Aspects of High-Resolution NMR of Bulk Polymers*, In: *High Resolution NMR Spectroscopy of Synthetic Polymers in Bulk*, R. A. Komoroski, Ed., VCH Verlagsgesellschaft, 1986, pp. 19–62.
8. B. Blümich and H. W. Spiess, *Angew. Chem.*, **100**, 1716–1734 (1988).
9. K. Schmidt-Rohr, *Hochauflösende Protonen-NMR an Festkörpern und Untersuchung der Phasenstruktur fester Polymere*, Diplomarbeit, Mainz, 1989.
10. S. P. Pappas, B. C. Pappas, L. R. Gatechair, and J. H. Jilek, *Polym. Photochem.*, **5**, 1 (1988).
11. S. Penczek, P. Kubisa, and R. Szymanski, *Makromol. Chem. V; Macromol. Symp.*, **3**, 203–220 (1986).
12. N. Bloembergen, *Physica*, **15**, 386–426 (1949).
13. D. L. VanderHart and A. N. Garroway, *J. Chem. Phys.*, **71**, 2773–2787 (1979).
14. E. O. Stejskal, J. Schaefer, M. D. Sefcik, and R. A. Mc Kay, *Macromolecules*, **14**, 275–279 (1981).
15. T. T. P. Cheung and B. C. Gerstein, *J. Appl. Phys.*, **52**, 5517–5528 (1981).
16. P. Caravatti, J. A. Deli, G. Bodenhausen, and R. R. Ernst, *J. Am. Chem. Soc.*, **104**, 5506–5507 (1982).
17. N. M. Szeverenyi, M. J. Sullivan, and G. E. Maciel, *J. Magn. Reson.*, **47**, 462–475 (1982).
18. K. J. Packer, J. M. Pope, and R. R. Yeung, *J. Polym. Sci.*, **22**, 589–616 (1984).
19. M. Linder, P. M. Henrichs, J. M. Hewitt, and D. J. Massa, *J. Chem. Phys.*, **82**, 1585–1598 (1985).
20. L. A. Belfiore and A. A. Patwardhan, *Polym. Mater. Sci. Eng.*, **54**, 638–644 (1986).
21. P. Caravatti, P. Neuenschwander, and R. R. Ernst, *Macromolecules*, **19**, 1889–1895 (1986).
22. I. J. Colquhoun and K. J. Packer, *Br. Polym. J.*, **19**, 151–163 (1987).
23. X. Zhang and Y. Wang, *Polymer*, **30**, 1867–1871 (1989).
24. P. Tekely, D. Canet, and J.-J. Delpuech, *Molecular Phys.*, **67**, 81–96 (1989).
25. K. Schmidt-Rohr, J. Clauss, B. Blümich, and H. W. Spiess, *Magn. Reson. Chemistry*, September (1990).
26. T. T. P. Cheung, *J. Chem. Phys.*, **76**, 1248–1254 (1982).
27. T. T. P. Cheung, *Phys. Rev. B*, **23**, 1404–1418 (1981).
28. I. J. Lowe and S. Gade, *Phys. Rev.*, **156**, 817–825 (1967).
29. R. A. Assink, *Macromolecules*, **11**, 1233–1237 (1978).
30. M. Goldman and L. Shen, *Phys. Rev.*, **144**, 321–331 (1966).
31. N. Zumbulyadis, *J. Magn. Reson.*, **53**, 486–494 (1983).
32. K. J. Packer and J. M. Pope, *J. Magn. Reson.*, **55**, 378–385 (1983).
33. K. Schmidt-Rohr, Ph.D. Thesis, Mainz, 1991.

Received January 16, 1991

Accepted February 25, 1991